PERGAMON Mathematical and Computer Modelling 0 (2004) 1–0
www.elsevier.com/locate/mcm

Global Maximum Norm Parameter-Uniform Numerical Method for a Singularly Perturbed Convection-Diffusion Problem with Discontinuous Convection Coefficient

P. A. Farrell
Department of Computer Science, Kent State University
Kent, OH 44242, U.S.A.
A. F. Hegarty
Department of Mathematics and Statistics, University of Limerick, Ireland
J. J. H. Miller
Department of Mathematics, Trinity College, Dublin, Ireland
E. O'Riordan
School of Mathematical Sciences, Dublin City University, Ireland
G. I. Shishkin
Institute for Mathematics and Mechanics, Russian Academy of Sciences, Ekaterinburg, Russia

Abstract—A singularly perturbed convection-diffusion problem, with a discontinuous convection coefficient and a singular perturbation parameter ε, is examined. Due to the discontinuity an interior layer appears in the solution. A finite difference method is constructed for solving this problem, which generates ε-uniformly convergent numerical approximations to the solution. The method uses a piecewise uniform mesh, which is fitted to the interior layer, and the standard upwind finite difference operator on this mesh. The main theoretical result is the ε-uniform convergence in the global maximum norm of the approximations generated by this finite difference method. Numerical results are presented, which are in agreement with the theoretical results.

Keywords—Singularly perturbed ODE, Discontinuous coefficient, Interior layer, Difference scheme, Piecewise-uniform mesh.

1. INTRODUCTION

Singularly perturbed differential equations arise in many branches of science and engineering [1]. Boundary and interior layers are normally present in the solutions of problems involving such equations. These layers are thin regions in the domain where the gradient of the solution steepens as the singular perturbation parameter tends to zero. The convergence of the numerical approximations generated by standard numerical methods applied to such problems depends adversely on the singular perturbation parameter [2–4]. Robust parameter-uniform numerical methods,

This research was supported in part by the Russian Foundation for Basic Research under Grant No. 01-01-01022, by the National Science Foundation Grant DMS-9627244, and by the Enterprise Ireland Grant SC-98-612.

0895-7177/04/$ - see front matter Typeset by $\mathcal{AMS}$-TEX
PII:00

with maximum norm errors independent of the singular perturbation parameter, have been developed over the last twenty years (see [2–4] and the references therein). Most of this work has concentrated on problems having only boundary layers in their solutions. Note that problems with discontinuous data were treated theoretically, in the case of the reaction-diffusion equation in, for example, [5]. The analytical techniques developed there are extended in a natural way to the problems considered in the present paper. In [6], we also examined the behaviour of the error for a class of singularly perturbed reaction-diffusion problems with interior layers. In a companion paper [7], we analyzed robust numerical methods for convection-diffusion problems with weak interior layers.

Here, we develop and analyze parameter-uniform numerical methods for a class of singularly perturbed convection-diffusion problems, whose solutions contain strong interior layers caused by a discontinuity in the convection coefficient. More specifically, we are concerned with a two point boundary value problem for a singularly perturbed convection diffusion equation with a singular perturbation parameter ε. The novel aspect of the problem under consideration is that the convection coefficient in the differential equation has a jump discontinuity at one or more points in the interior of the domain. This gives rise to an interior layer in the exact solution of the problem. Our goal is to construct an ε-uniform numerical method for solving this problem, by which we mean a numerical method which generates ε-uniformly convergent numerical approximations to the solution.

We now outline the main points of the paper. In the next section, we describe the problem and establish the existence and regularity of its solutions. We state and prove a comparison principle and some *a priori* estimates of the solution and its derivatives. Then, we prove a stability result from which the uniqueness of the solution follows. We decompose this solution into smooth and singular components and establish ε-explicit bounds on these components and their derivatives. In Section 3, we construct a piecewise uniform mesh, which is fitted to the interior layers. The numerical method is defined by using the standard upwind finite difference method on this mesh. We state and prove a comparison principle and a stability result for the discrete problem. We introduce a decomposition of the discrete solution in Section 4 and prove the main theoretical result, namely the ε-uniform convergence in the global maximum norm of the approximations generated by the finite difference method. In the following section, numerical results are presented, which are in agreement with the theoretical results. The paper ends with a section containing the conclusions.

2. CONTINUOUS PROBLEM

A singularly perturbed convection-diffusion equation in one dimension with a discontinuous coefficient of the first derivative term is considered on the unit interval $\Omega = (0,1)$. A single discontinuity in the coefficient is assumed to occur at a point $d \in \Omega$. It is convenient to introduce the notation $\Omega^- = (0,d)$ and $\Omega^+ = (d,1)$ and to denote the jump at d in any function with $[\omega](d) = \omega(d+) - \omega(d-)$. The corresponding two point boundary value problem is as follows. Find $u_\varepsilon \in C^1(\Omega) \cap C^2(\Omega^- \cup \Omega^+)$, such that

$$\begin{gathered}
\varepsilon u_\varepsilon'' + a(x)u_\varepsilon' = f, \qquad \text{for all } x \in \Omega^- \cup \Omega^+, \\
u_\varepsilon(0) = u_0, \qquad u_\varepsilon(1) = u_1, \\
a(x) < -\alpha_1 < 0, \qquad x < d, \qquad a(x) > \alpha_2 > 0, \qquad x > d, \\
|[a](d)| \le C, \qquad |[f](d)| \le C,
\end{gathered} \tag{P_ε}$$

where $a, f \in C^2(\Omega^- \cup \Omega^+)$; these functions are extendable into $\overline{\Omega^-}$ and $\overline{\Omega^+}$ in C^2. Note the level of smoothness required of the solution, i.e., $u_\varepsilon \in C^1(\Omega)$. Throughout this paper, C denotes a generic positive constant that is independent of the singular perturbation parameter ε and of N, the dimension of the discrete problem. We measure all functions in the maximum pointwise norm, which we denote by

$$\|w\|_D = \sup_{x \in D} |w(x)|.$$

When the domain is obvious, we will omit the subscript in this notation.

Note the sign pattern of the coefficient a of the first derivative, which is negative to the left of the point of discontinuity and positive to the right of this point. In general, there is an interior layer in the vicinity of the point of discontinuity $x = d$.

Theorem 1. *Problem* (P_ε) *has a solution* $u_\varepsilon \in C^1(\Omega) \cap C^2(\Omega^- \cup \Omega^+)$.

Proof. The proof is by construction. Let y_1, y_2 be particular solutions of the differential equations

$$\varepsilon y_1'' + a_1(x) y_1' = f, \quad x \in \Omega^-, \qquad \text{and} \qquad \varepsilon y_2'' + a_2(x) y_2' = f, \quad x \in \Omega^+,$$

where $a_1, a_2 \in C^2(\Omega)$ with the following properties:

$$\begin{aligned} a_1(x) &= a(x), \quad x \in \Omega^-, \qquad a_1 < 0, \quad x \in \Omega, \\ a_2(x) &= a(x), \quad x \in \Omega^+, \qquad a_2 > 0, \quad x \in \Omega. \end{aligned}$$

Consider the function

$$y(x) = \begin{cases} y_1(x) + (u_\varepsilon(0) - y_1(0))\phi_1(x) + A\phi_2(x), & x \in \Omega^-, \\ y_2(x) + B\phi_1(x) + (u_\varepsilon(1) - y_2(1))\phi_2(x), & x \in \Omega^+, \end{cases}$$

where $\phi_1(x)$, $\phi_2(x)$ are the solutions of the boundary value problems

$$\begin{aligned} \varepsilon\phi_1'' + a_1(x)\phi_1' &= 0, \quad x \in \Omega, \qquad \phi_1(0) = 1, \quad \phi_1(1) = 0, \\ \varepsilon\phi_2'' + a_2(x)\phi_2' &= 0, \quad x \in \Omega, \qquad \phi_2(0) = 0, \quad \phi_2(1) = 1. \end{aligned}$$

Any function of this form satisfies $y(0) = u_\varepsilon(0)$, $y(1) = u_\varepsilon(1)$, and $\varepsilon y'' + a(x)y' = f$, $x \in \Omega^- \cup \Omega^+$. Note that on the open interval $(0,1)$, $0 < \phi_i < 1$, $i = 1, 2$. Thus, ϕ_1, ϕ_2 cannot have an internal maximum or minimum and hence

$$\phi_1' < 0, \quad \phi_2' > 0, \qquad x \in (0,1).$$

We wish to choose the constants A, B so that $y \in C^1(\Omega)$. That is, we impose

$$y(d^-) = y\left(d^+\right) \qquad \text{and} \qquad y'(d^-) = y'\left(d^+\right).$$

For the constants A, B to exist we require that

$$\begin{bmatrix} \phi_2(d) - \phi_1(d) \\ \phi_2'(d) - \phi_1'(d) \end{bmatrix} \neq 0.$$

This follows from observing that $\phi_2'(d)\phi_1(d) - \phi_2(d)\phi_1'(d) > 0$.

Note that there will also be a solution to convection-diffusion problems with a discontinuous coefficient of the first derivative, when the coefficient $a(x)$ has other sign patterns either side of the discontinuity. For example, if $a(d^+) \neq a(d^-)$ and $a(x) > 0$, $x \in \Omega$, then a weak interior layer occurs to the right of $x = d$ and a boundary layer occurs near $x = 0$. Similarly, if $a(d^+) \neq a(d^-)$ and $a(x) < 0$, $x \in \Omega$, then a weak interior layer occurs to the left of $x = d$ and a boundary layer occurs near $x = 1$. These weak interior layers have been examined in [7]. On the other hand, if the sign of $a(x)$ changes at $x = d$, for example, if $a(x) \geq \alpha_1 > 0$, $x \in \Omega^-$, and $a(x) \leq \alpha_2 < 0$, $x \in \Omega^+$, then, in general, the solution is not bounded independently of ε. We illustrate this case by considering the following constant coefficient problem.

Find $u_\varepsilon \in C^1(\Omega)$, such that

$$\varepsilon u_\varepsilon'' + u_\varepsilon' = -1, \quad x < 0.5, \qquad \varepsilon u_\varepsilon'' - u_\varepsilon' = -1, \quad x > 0.5, \qquad u_\varepsilon(0) = u_\varepsilon(1) = 0.$$

Its solution has the value $u_\varepsilon(0.5) = -0.5 + \varepsilon e^{1/(2\varepsilon)}(1 - e^{-1/(2\varepsilon)})$, which becomes unbounded as $\varepsilon \to 0$. We do not discuss such cases in greater detail in this paper.

Let L_ε denote the differential operator occurring in (P_ε), which is defined as

$$L_\varepsilon \omega \equiv \varepsilon\omega'' + a(x)\omega'.$$

Then, L_ε satisfies the following comparison principle on $\bar{\Omega}$.

Lemma 2. *Suppose that a function $\omega \in C^0(\bar{\Omega}) \cap C^2(\Omega^- \cup \Omega^+)$ satisfies*

$$\begin{aligned} \omega(0) \le 0, \quad \omega(1) \le 0, \qquad & [\omega'](d) \ge 0, \\ L_\varepsilon \omega(x) \ge 0, \qquad & \textit{for all } x \in \Omega^- \cup \Omega^+, \qquad \textit{then} \\ \omega(x) \le 0, \qquad & \textit{for all } x \in \bar{\Omega}. \end{aligned}$$

Proof. We introduce the function $v(x)$, defined by

$$\omega(x) = e^{-(\alpha(x)|x-d|)/(2\varepsilon)} v(x),$$

where $\alpha(x) = \alpha_1$, $x < d$, $\alpha(x) = \alpha_2$, $x > d$. Hence, for $x \in \Omega^-$,

$$L_\varepsilon \omega = e^{-(\alpha(x)|x-d|)/(2\varepsilon)} \left(\varepsilon v'' + (a + \alpha_1) v' + \frac{\alpha_1}{2\varepsilon} \left(\frac{\alpha_1}{2} + a \right) v \right),$$

and for $x \in \Omega^+$

$$L_\varepsilon \omega = e^{-(\alpha(x)|x-d|)/(2\varepsilon)} \left(\varepsilon v'' + (a - \alpha_2) v' + \frac{\alpha_2}{2\varepsilon} \left(\frac{\alpha_2}{2} - a \right) v \right).$$

Let q be a point at which v attains its maximum value in $\bar{\Omega}$. If $v(q) \le 0$, there is nothing to prove. Suppose therefore that $v(q) > 0$, then the proof is completed by showing that this leads to a contradiction. With the above assumption on the boundary values, either $q \in \Omega^- \cup \Omega^+$ or $q = d$. If $q \in \Omega^-$ then

$$L_\varepsilon \omega(q) = e^{-(\alpha_1(d-q))/(2\varepsilon)} \left(\varepsilon v''(q) + (a(q) + \alpha_1) v'(q) + \frac{\alpha_1}{2\varepsilon} \left(\frac{\alpha_1}{2} + a \right) v(q) \right) < 0,$$

which is a contradiction. If $q \in \Omega^+$ then

$$L_\varepsilon \omega(q) = e^{-(\alpha_2(q-d))/(2\varepsilon)} \left(\varepsilon v''(q) + (a(q) - \alpha_2) v'(q) + \frac{\alpha_2}{2\varepsilon} \left(\frac{\alpha_2}{2} - a \right) v(q) \right) < 0,$$

which is also a contradiction.

The only possibility remaining is that $q = d$. Note that $[v](d) = [\omega](d) = 0$ and $[\omega'](d) = [v'](d) - ((\alpha_1 + \alpha_2)/(2\varepsilon)) v(d)$. Since d is where v takes its maximum value, then $v'(d-) \ge 0$, $v'(d+) \le 0$, which implies that $[v'](d) \le 0$. This implies that $[\omega'](d) < 0$, which is a contradiction.

An immediate consequence of the comparison principle is the following stability result, which implies uniqueness of the solution.

Theorem 3. *Let u_ε be a solution of (P_ε), then*

$$\|u_\varepsilon\|_{\bar{\Omega}} \le \max\{|u_0|, |u_1|\} + \frac{1}{\gamma} \|f\|_{\bar{\Omega}},$$

where $\gamma = \min\{\alpha_1/d, \alpha_2/(1-d)\}$.

Proof. Put $\Psi_\pm(x) = -M - (x\|f\|)/(\gamma d) \pm u_\varepsilon(x)$, $x \le d$, and $\Psi_\pm(x) = -M - ((1-x)\|f\|)/(\gamma(1-d)) \pm u_\varepsilon(x)$, $x > d$, where $M = \max\{|u_0|, |u_1|\}$. Then, clearly $\Psi_\pm \in C^0(\bar{\Omega})$, $\bar{\Psi}_\pm(0) \le 0$, $\Psi_\pm(1) \le 0$, and for each $x \in \Omega^- \cup \Omega^+$

$$L_\varepsilon \Psi_\pm(x) \ge 0.$$

Furthermore, since $u_\varepsilon \in C^1(\Omega)$

$$[\Psi_\pm](d) = \pm[u_\varepsilon](d) = 0, \qquad \text{and} \qquad [\Psi'_\pm](d) = \frac{\|f\|}{\gamma(1-d)} + \frac{\|f\|}{\gamma d} \ge 0.$$

It follows from the comparison principle given in the previous lemma that $\Psi_\pm(x) \le 0$ for all $x \in \bar{\Omega}$, which leads at once to the desired bound on u_ε.

Consider the following decomposition of the solution $u_\varepsilon = v_\varepsilon + w_\varepsilon$ into a nonlayer component v_ε and an interior layer component w_ε. Define the discontinuous functions v_0 and v_1 by

$$\begin{aligned} a v_0' &= f, & x &\in \Omega^- \cup \Omega^+, \\ v_0(0) &= u_\varepsilon(0), & v_0(1) &= u_\varepsilon(1), \\ a v_1' &= -v_0'', & x &\in \Omega^- \cup \Omega^+, \\ v_1(0) &= 0, & v_1(1) &= 0. \end{aligned}$$

We now define the discontinuous function v_ε by

$$L_\varepsilon v_\varepsilon = f, \qquad x \in \Omega^- \cup \Omega^+, \tag{2.1a}$$

$$v_\varepsilon(0) = u_\varepsilon(0), \qquad v_\varepsilon(d^-) = v_0(d^-) + \varepsilon v_1(d^-), \tag{2.1b}$$

$$v_\varepsilon\left(d^+\right) = v_0\left(d^+\right) + \varepsilon v_1\left(d^+\right), \qquad v_\varepsilon(1) = u_\varepsilon(1). \tag{2.1c}$$

Define the discontinuous function w_ε, which is the layer component of the decomposition, as follows:

$$L_\varepsilon w_\varepsilon = 0, \qquad x \in \Omega^- \cup \Omega^+, \tag{2.2a}$$

$$w_\varepsilon(0) = w_\varepsilon(1) = 0, \qquad [w_\varepsilon](d) = -[v_\varepsilon](d), \qquad [w_\varepsilon'](d) = -[v_\varepsilon'](d). \tag{2.2b}$$

Hence, $w_\varepsilon(d^-) = u_\varepsilon(d^-) - v_\varepsilon(d^-)$ and $w_\varepsilon(d^+) = u_\varepsilon(d^+) - v_\varepsilon(d^+)$. Note that since there is a unique solution to (P_ε), then $u_\varepsilon = v_\varepsilon + w_\varepsilon$. It is also worth noting that both v_ε and w_ε are discontinuous at $x = d$, but by (2.2b) their sum is in $C^1(\Omega)$.

LEMMA 4. *For each integer k, satisfying $0 \le k \le 3$, the solutions v_ε and w_ε of (2.1) and (2.2), respectively, satisfy the following bounds:*

$$\|v_\varepsilon\| \le C, \qquad \left\|v_\varepsilon^{(k)}\right\|_{\Omega^- \cup \Omega^+} \le C\left(1 + \varepsilon^{2-k}\right),$$

$$|[v_\varepsilon](d)|, \left|\left[v_\varepsilon'\right](d)\right|, \left|\left[v_\varepsilon''\right](d)\right| \le C,$$

$$\left|w_\varepsilon^{(k)}(x)\right| \le \begin{cases} C\left(\varepsilon^{-k} e^{-(d-x)\alpha_1/\varepsilon}\right), & x \in \Omega^-, \\ C\left(\varepsilon^{-k} e^{-(x-d)\alpha_2/\varepsilon}\right), & x \in \Omega^+, \end{cases}$$

where C is a constant independent of ε.

PROOF. Apply the arguments given in [3, Chapter 3] separately on each of the subintervals Ω^- and Ω^+.

Note that w_ε is a discontinuous function which is increasing exponentially (decreasing exponentially) to the left (to the right) of the point $x = d$.

3. DISCRETE PROBLEM

A fitted mesh method for problem (P_ε) is now introduced (see [3] for motivation for this choice of mesh). On Ω a piecewise-uniform mesh of N mesh intervals is constructed as follows. The domain $\bar{\Omega}$ is subdivided into the four subintervals

$$[0, d - \sigma_1] \cup [d - \sigma_1, d] \cup [d, d + \sigma_2] \cup [d + \sigma_2, 1], \tag{3.1a}$$

for some σ_1, σ_2 that satisfy $0 < \sigma_1 \le d/2$, $0 < \sigma_2 \le (1-d)/2$. On each subinterval a uniform mesh with $N/4$ mesh-intervals is placed. The interior points of the mesh are denoted by

$$\Omega_\varepsilon^N = \left\{x_i : 1 \le i \le \frac{N}{2} - 1\right\} \cup \left\{x_i : \frac{N}{2} + 1 \le i \le N - 1\right\}. \tag{3.1b}$$

Clearly, $x_{N/2} = d$ and $\bar{\Omega}_\varepsilon^N = \{x_i\}_0^N$.

Note that this mesh is a uniform mesh when $\sigma_1 = d/2$ and $\sigma_2 = (1-d)/2$. It is fitted to the singular perturbation problem (P_ε) by choosing σ_1 and σ_2 to be the following functions of N and ε:

$$\sigma_1 = \min\left\{\frac{d}{2}, \frac{\varepsilon}{\alpha}\ln N\right\}, \qquad \sigma_2 = \min\left\{\frac{1-d}{2}, \frac{\varepsilon}{\alpha}\ln N\right\}, \tag{3.1c}$$

where

$$\alpha = \min\{\alpha_1, \alpha_2\}. \tag{3.1d}$$

REMARK. An alternative choice of transition points would be

$$\hat{\sigma}_1 = d\min\left\{\frac{1}{2}, \frac{\varepsilon}{\alpha_1}\ln N\right\}, \qquad \hat{\sigma}_2 = (1-d)\min\left\{\frac{1}{2}, \frac{\varepsilon}{\alpha_2}\ln N\right\}.$$

The analysis which follows is also applicable to this choice of transition parameters.

On the piecewise-uniform mesh $\bar{\Omega}^N_\varepsilon$ a standard upwind finite difference operator is used. Then, the fitted mesh method for (P_ε) is as follows.

Find a mesh function U_ε, such that

$$\begin{gathered} L^N_\varepsilon U_\varepsilon \equiv \varepsilon\delta^2 U_\varepsilon(x_i) + a(x_i)DU_\varepsilon(x_i) = f(x_i), \qquad \text{for all } x_i \in \Omega^N_\varepsilon, \\ U_\varepsilon(0) = u_0, \qquad U_\varepsilon(1) = u_1, \\ D^- U_\varepsilon\left(x_{N/2}\right) = D^+ U_\varepsilon\left(x_{N/2}\right), \end{gathered} \tag{P^N_ε}$$

where

$$\delta^2 Z_i = \frac{2\left(D^+ Z_i - D^- Z_i\right)}{x_{i+1} - x_{i-1}}, \qquad \text{and} \qquad DZ_i = \begin{cases} D^- Z_i, & i < \dfrac{N}{2}, \\ D^+ Z_i, & i > \dfrac{N}{2}, \end{cases}$$

where D^+ and D^- are the standard forward and backward finite difference operators, respectively. The following lemma shows that the finite difference operator L^N_ε has properties analogous to those of the differential operator L_ε.

LEMMA 5. *Suppose that a mesh function Z satisfies*

$$\begin{aligned} &Z(0) \le 0, \quad Z(1) \le 0, \quad L^N_\varepsilon Z(x_i) \ge 0, \qquad \textit{for all } x_i \in \Omega^N_\varepsilon, \quad \textit{and} \\ &D^+Z(d) - D^-Z(d) \ge 0, \qquad \textit{then } Z(x_i) \le 0, \qquad \textit{for all } x_i \in \bar{\Omega}^N_\varepsilon. \end{aligned}$$

PROOF. Let x_p be any point at which $Z(x_p)$ attains its maximum value on $\bar{\Omega}^N_\varepsilon$. If $Z(x_p) \le 0$ there is nothing to prove. Suppose therefore that $Z(x_p) > 0$, then the proof is completed by showing that this leads to a contradiction. By the assumptions, $x_p \ne 0, 1$. Consider first the case of $x_p \ne d$. Without loss of generality, assume $x_p < d$. Because Z attains its maximum value at x_p it is clear that

$$D^- Z(x_p) \ge 0 \ge D^+ Z(x_p),$$

and hence

$$L^N_\varepsilon Z(x_p) = \varepsilon\delta^2 Z(x_p) + a(x_p)D^- Z(x_p) \le 0.$$

To avoid a contradiction, $L^N_\varepsilon Z(x_p) = 0$. This implies that

$$Z(x_{p-1}) = Z(x_p) = Z(x_{p+1}).$$

Repeat the argument at the point x_{p-1}. Continue until the boundary point x_0 is reached and a contradiction is achieved. Let us now consider the case of $x_p = d$. Then,

$$D^- Z(d) \ge 0 \ge D^+ Z(d) \ge D^- Z(d),$$

and so

$$Z\left(x_{N/2-1}\right) = Z(d) = Z\left(X_{N/2+1}\right).$$

Repeat earlier argument to reach the desired contradiction. ∎

LEMMA 6. *If U_ε is the solution of* $(\mathrm{P}_\varepsilon^N)$, *then*

$$|U_\varepsilon(x_i)| \le C, \qquad \forall\, x_i \in \bar{\Omega}_\varepsilon^N,$$

where C is a constant independent of ε and N.

PROOF. The proof is the discrete analogue of the continuous stability bound given in Theorem 3. ∎

4. ERROR ANALYSIS

To bound the nodal error $|(U_\varepsilon - u_\varepsilon)(x_i)|$, the argument is divided into two main parts. Initially, we define mesh functions V_L and V_R, which approximate v_ε, respectively, to the left and to the right of the point of discontinuity $x = d$. Then, we construct mesh functions W_L and W_R (to approximate w_ε on either side of $x = d$) so that the amplitude of the jump $W_R(d) - W_L(d)$ is determined by the size of the jump $|[v_\varepsilon](d)|$. Also W_L and W_R are sufficiently small away from the interior layer region. Using these mesh functions the nodal error $|(U_\varepsilon - u_\varepsilon)(x_i)|$ is then bounded separately outside and inside the layer.

Define the mesh functions V_L and V_R to be the solutions of the following discrete problems:

$$L_\varepsilon^N V_L = f(x_i), \qquad \text{for all } x_i \in \Omega_\varepsilon^N \cap \Omega^-, \tag{4.1a}$$
$$V_L(0) = v_\varepsilon(0), \qquad V_L(d) = v_\varepsilon(d^-), \tag{4.1b}$$

and

$$L_\varepsilon^N V_R = f(x_i), \qquad \text{for all } x_i \in \Omega_\varepsilon^N \cap \Omega^+, \tag{4.1c}$$
$$V_R(1) = v_\varepsilon(1), \qquad V_R(d) = v_\varepsilon\left(d^+\right). \tag{4.1d}$$

Using the following barrier functions, separately, on the appropriate sides of the discontinuity,

$$-C\frac{x_i N^{-1}}{d}, \qquad -C\frac{(1-x_i)N^{-1}}{1-d},$$

one can easily deduce (see [3]) the following error bounds:

$$|V_L(x_i) - v_\varepsilon(x_i)| \le CN^{-1}x_i, \qquad x_i \in \Omega_\varepsilon^N \cap \Omega^-, \tag{4.2a}$$
$$|V_R(x_i) - v_\varepsilon(x_i)| \le CN^{-1}(1-x_i), \qquad x_i \in \Omega_\varepsilon^N \cap \Omega^+. \tag{4.2b}$$

Define the mesh functions $W_L : \bar{\Omega}_\varepsilon^N \cap [0,d] \to R$ and $W_R : \bar{\Omega}_\varepsilon^N \cap [d,1] \to R$ to be the solutions of the following system of finite difference equations:

$$L_\varepsilon^N W_L = 0, \qquad \text{for all } x_i \in \Omega_\varepsilon^N \cap \Omega^-, \tag{4.3a}$$
$$L_\varepsilon^N W_R = 0, \qquad \text{for all } x_i \in \Omega_\varepsilon^N \cap \Omega^+, \tag{4.3b}$$
$$W_L(0) = 0, \qquad W_R(1) = 0, \tag{4.3c}$$
$$W_R(d) + V_R(d) = W_L(d) + V_L(d), \tag{4.3d}$$
$$D^+W_R(d) + D^+V_R(d) = D^-W_L(d) + D^-V_L(d). \tag{4.3e}$$

Note that we can define U_ε to be

$$U_\varepsilon(x_i) = \begin{cases} V_L(x_i) + W_L(x_i), & x_i \in \Omega_\varepsilon^N \cap \Omega^-, \\ V_L(d) + W_L(d) = V_R(d) + W_R(d), & x_i = d, \\ W_R(x_i) + V_R(x_i), & x_i \in \Omega_\varepsilon^N \cap \Omega^+. \end{cases}$$

By Lemma 6 $|U_\varepsilon(d)| \le C$ and with Theorem 3, one easily deduces that

$$|W_L(d)| \le C \qquad \text{and} \qquad |W_R(d)| \le C.$$

Observe that W_L (W_R) satisfies a homogeneous difference equation (4.3a) ((4.3b)) and that $W_L(0) = 0$ ($W_R(1) = 0$). From the arguments in [3, Chapter 3], for $x_i \le d - \sigma_1$ and, respectively, $x_i \ge d + \sigma_2$, we have

$$|W_L(x_i)| \le |W_L(d)|N^{-1} \le CN^{-1}, \qquad |W_R(x_i)| \le |W_R(d)|N^{-1} \le CN^{-1}, \tag{4.4}$$

when $\sigma_1 = \sigma_2 = (\varepsilon/\gamma)\ln N$. For $x_i \le d - \sigma_1$ and $\sigma_1 = (\varepsilon/\alpha)\ln N$, we then have the error bound

$$|W_L(x_i) - w_\varepsilon(x_i)| \le |W_L(x_i)| + |w_\varepsilon(x_i)| \le |W_L(d)|N^{-1} + Ce^{-\alpha\sigma_1/\varepsilon} \le CN^{-1}. \tag{4.5a}$$

Similarly, for $x_i \ge d + \sigma_2$ and $\sigma_2 = (\varepsilon/\alpha)\ln N$, we obtain

$$|W_R(x_i) - w_\varepsilon(x_i)| \le CN^{-1}. \tag{4.5b}$$

We now state and prove the main theoretical result in this paper.

Theorem 7. *The solutions u_ε and U_ε of (P_ε) and $(\mathrm{P}_\varepsilon^N)$ satisfy the following bound:*

$$\left\|\bar{U}_\varepsilon - u_\varepsilon\right\|_{\bar{\Omega}} \le CN^{-1}(\ln N)^2,$$

where $\bar{U}_\varepsilon$ is the piecewise linear interpolant of U_ε on $\bar{\Omega}$ and C is a constant independent of N and ε.

Proof. Consider first the case of $\sigma_1 = \sigma_2 = \sigma = (\varepsilon/\alpha)\ln N$. From (4.5) and the bounds (4.2), it follows that

$$|U_\varepsilon(d-\sigma) - u_\varepsilon(d-\sigma)| \le CN^{-1}, \qquad |U_\varepsilon(d+\sigma) - u_\varepsilon(d+\sigma)| \le CN^{-1}. \tag{4.6}$$

Note that for $x_i \in (d-\sigma, d+\sigma) \setminus \{d\}$, using the bounds on the derivatives given in Lemma 4, we have that

$$\left|L_\varepsilon^N(U_\varepsilon - u_\varepsilon)\right| \le \varepsilon h \left|u_\varepsilon^{(3)}\right| + h\left|u_\varepsilon^{(2)}\right| \le C\frac{h}{\varepsilon^2},$$

where $h = (4\sigma)/N$ is the fine mesh size. At the mesh point $x_i = d$,

$$\begin{aligned}\left|\left(D^+ - D^-\right)(U_\varepsilon - u_\varepsilon)\right| &= \left|\left(D^- - D^+\right)(u_\varepsilon) + [u_\varepsilon']\right| \\ &\le \left|u_\varepsilon'(x_i) - D^+u_\varepsilon(x_i)\right| + \left|u_\varepsilon'(x_i) - D^-u_\varepsilon(x_i)\right| \le C\frac{h}{\varepsilon^2} = \frac{C\sigma}{\varepsilon^2 N}.\end{aligned}$$

Consider the discrete barrier function

$$\Psi = -CN^{-1} - C\frac{N^{-1}\sigma}{\varepsilon^2}\begin{cases} x_i - (d-\sigma), & x_i \in \Omega_\varepsilon^N \cap (d-\sigma, d), \\ (d+\sigma) - x_i, & x_i \in \Omega_\varepsilon^N \cap (d, d+\sigma). \end{cases}$$

Note that

$$L_\varepsilon^N \Psi = C\frac{N^{-1}\sigma}{\varepsilon^2}\begin{cases} -a, & x_i \in \Omega_\varepsilon^N \cap (d-\sigma, d), \\ a, & x_i \in \Omega_\varepsilon^N \cap (d, d+\sigma), \end{cases}$$

and

$$D^+\Psi(d) - D^-\Psi(d) = 2C\frac{N^{-1}\sigma}{\varepsilon^2}.$$

Applying the discrete comparison principle to $\Psi \pm (U_\varepsilon - u_\varepsilon)$ over the interval $[d-\sigma, d+\sigma]$, we get

$$|U_\varepsilon(x_i) - u_\varepsilon(x_i)| \le C\frac{N^{-1}\sigma^2}{\varepsilon^2} \le CN^{-1}(\ln N)^2.$$

We complete the proof by considering the case where at least one of the two transition points σ_1, σ_2 takes the value $d/2$ or $(1-d)/2$. In all such cases $\varepsilon^{-1} \le C \ln N$. Applying the discrete comparison principle across the entire domain Ω_ε^N, we have for $x_i \neq d$

$$\left|L_\varepsilon^N (U_\varepsilon - u_\varepsilon)\right| \le \varepsilon N^{-1} \left|u_\varepsilon^{(3)}\right| + N^{-1} \left|u_\varepsilon^{(2)}\right| \le C\frac{N^{-1}}{\varepsilon^2} \le CN^{-1}(\ln N)^2,$$

and

$$\left|\left(D^+ - D^-\right)(U_\varepsilon - u_\varepsilon)\right| = \left|-\left(D^+ - D^-\right)(u_\varepsilon) + [u'_\varepsilon]\right| \le C\frac{N^{-1}}{\varepsilon^2} \le CN^{-1}(\ln N)^2.$$

Use the barrier function

$$\Psi_1 = -CN^{-1}(\ln N)^2 \begin{cases} (1-d)x_i, & x_i \in \Omega_\varepsilon^N \cap (0,d), \\ d(1-x_i), & x_i \in \Omega_\varepsilon^N \cap (d,1), \end{cases}$$

to get the nodal error estimate

$$|(U_\varepsilon - u_\varepsilon)(x_i)| \le CN^{-1}(\ln N)^2, \qquad x_i \in \bar{\Omega}_\varepsilon^N.$$

Follow the arguments in [3, Section 3.4], applied separately on the intervals $[0,d]$ and $[d,1]$ to extend this to the global error bound

$$\left\|\bar{U}_\varepsilon - u_\varepsilon\right\|_\Omega \le CN^{-1}(\ln N)^2. \qquad \blacksquare$$

5. NUMERICAL EXAMPLE

Consider the particular problem

$$\varepsilon u''_\varepsilon + a(x)u'_\varepsilon = f, \tag{5.1a}$$

with the boundary conditions

$$u_\varepsilon(0) = 0, \qquad u_\varepsilon(1) = 1, \tag{5.1b}$$

where

$$a(x) = \begin{cases} -1, & 0 \le x \le 0.4, \\ 1, & 0.4 < x \le 1, \end{cases} \tag{5.1c}$$

and

$$f(x) = \begin{cases} -4x, & 0 \le x \le 0.25, \\ -1, & 0.25 < x \le 0.4, \\ 1, & 0.4 < x \le 0.5, \\ 2-2x, & 0.5 < x \le 1. \end{cases} \tag{5.1d}$$

This problem is solved numerically using $(\mathrm{P}_\varepsilon^N)$ and the fitted meshes Ω_ε^N defined in (3.3). Plots of the numerical solutions with $N = 32$ are shown for some values of ε in Figures 1–3, together with plots of the approximate global error in each case. The global error is approximated by the maximum pointwise difference between the numerical solution on the mesh Ω_ε^{32} and that on the mesh $\Omega_\varepsilon^{4096}$. That is,

$$E_{\varepsilon,\mathrm{nodal}}^N = \max_{x_i \in \Omega_\varepsilon^N} \left|U_\varepsilon^N - \bar{U}_\varepsilon^{4096}\right|,$$

$$E_{\varepsilon,\mathrm{global}}^N = \max_{x_i \in \Omega_\varepsilon^{4096}} \left|\bar{U}_\varepsilon^N - U_\varepsilon^{4096}\right|.$$

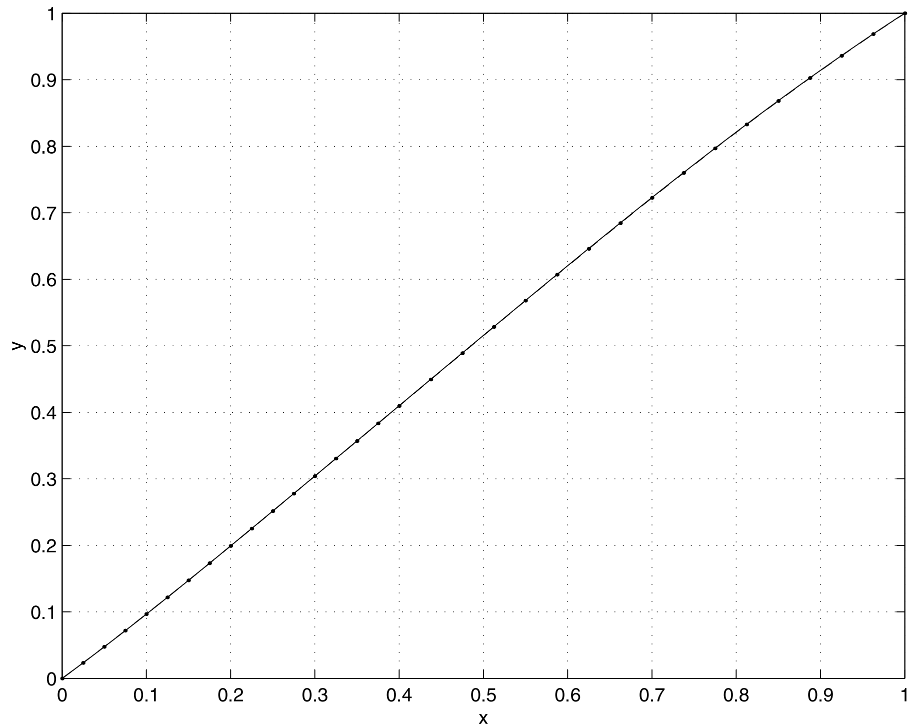

(a). U_1^{32} (- -), U_1^{4096} (—).

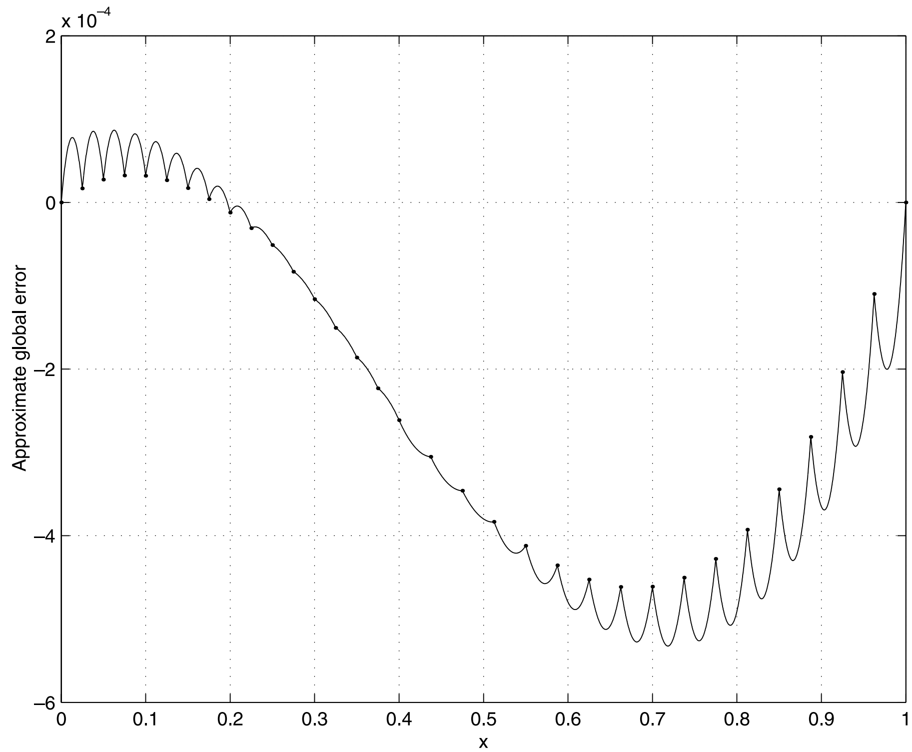

(b). $E^{32}_{\varepsilon=1,\mathrm{global}}$.

Figure 1. Plots of the numerical solution U_ε^N, the continuous solution u_ε, and approximate global error $E^N_{\varepsilon,\mathrm{global}}$, respectively, for $\varepsilon = 1$ and $N = 32$.

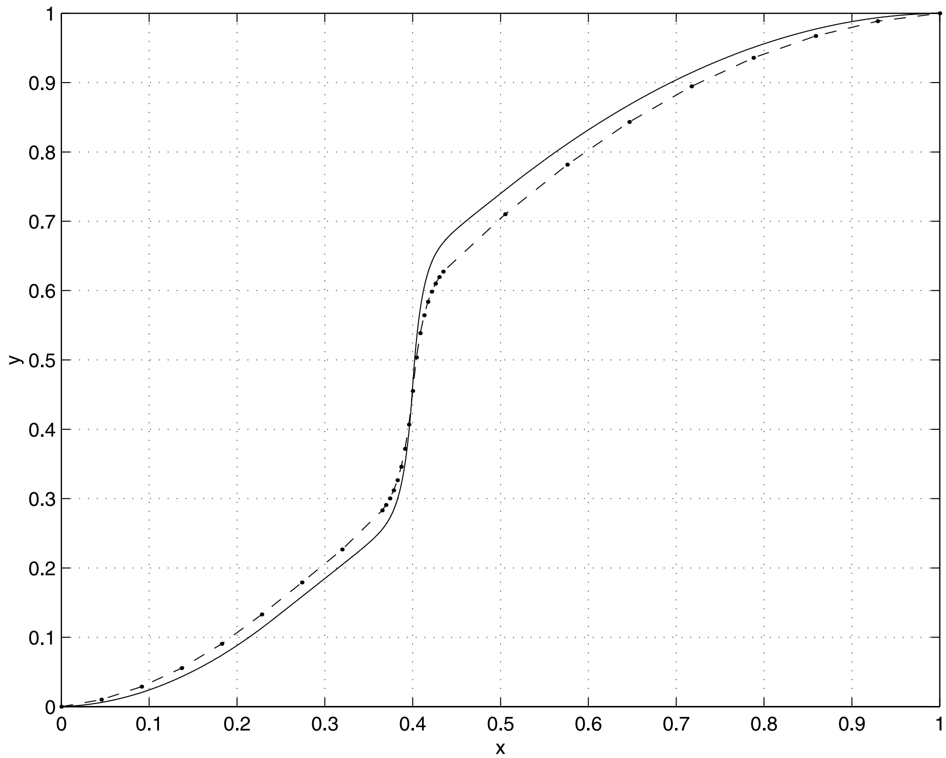

(a). $U^{32}_{0.01}$ (- -), $U^{4096}_{0.01}$ (—).

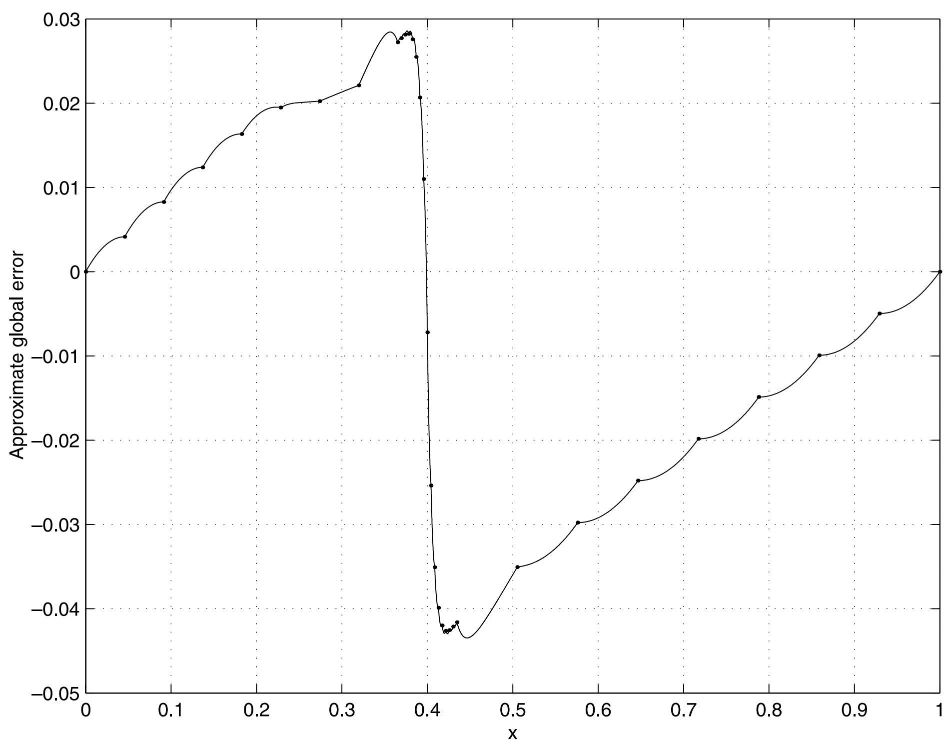

(b). $E^{32}_{\varepsilon=0.01,\mathrm{global}}$.

Figure 2. Plots of the numerical solution U^N_ε, the continuous solution u_ε, and approximate global error $E^N_{\varepsilon,\mathrm{global}}$, respectively, for $\varepsilon = 0.01$ and $N = 32$.

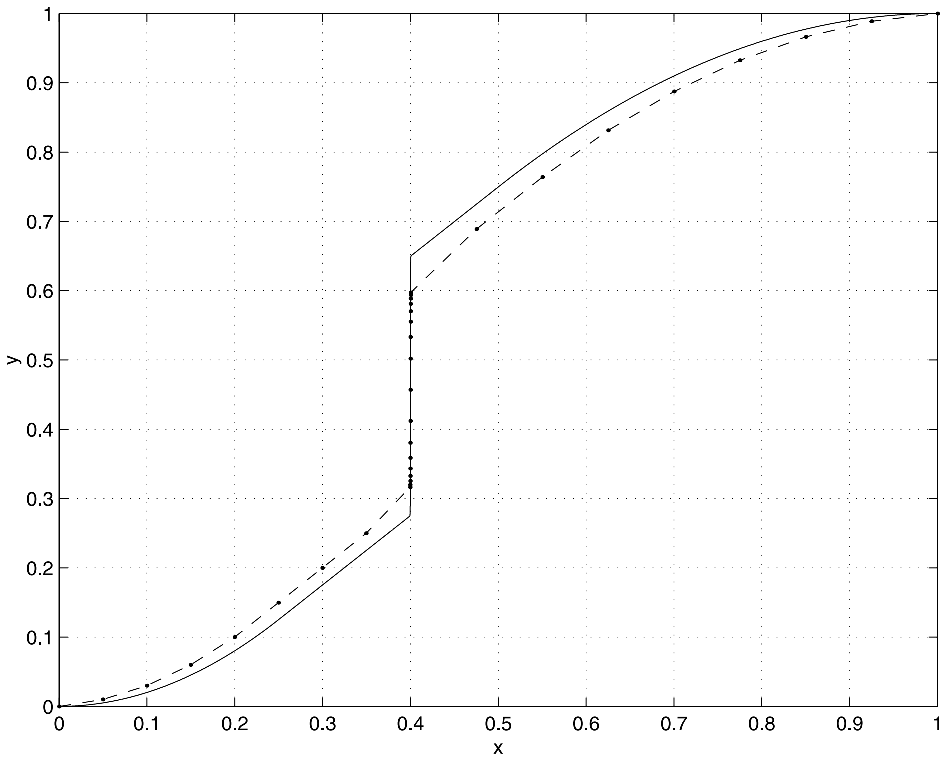

(a). $U^{32}_{0.0001}$ (- -), $U^{4096}_{0.0001}$ (—).

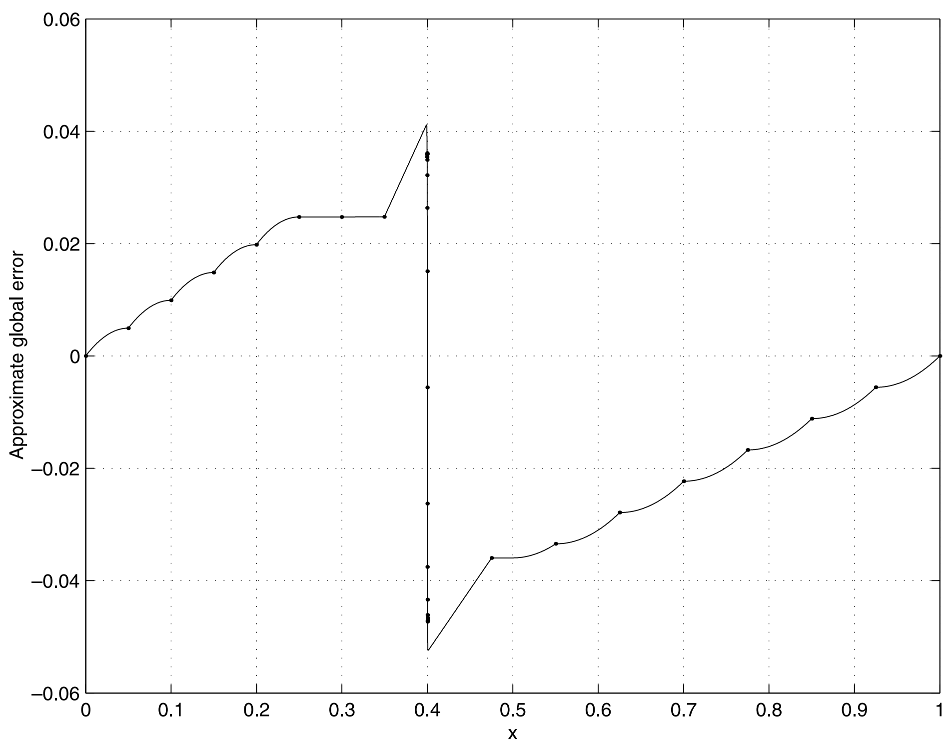

(b). $E^{32}_{\varepsilon=0.0001,\mathrm{global}}$.

Figure 3. Plots of the numerical solution U^N_ε, the continuous solution u_ε, and approximate global error $E^N_{\varepsilon,\mathrm{global}}$, respectively, for $\varepsilon = 0.0001$ and $N = 32$.

Table 1. Maximum pointwise errors $E^N_{\varepsilon,\text{nodal}}$ for the fitted mesh method $(\mathrm{P}^N_\varepsilon)$ applied to problem (5.1).

ε	Number of Intervals N			
	8	16	32	64
1	2.0830E − 3	9.1112E − 4	4.6146E − 4	2.3036E − 4
2^{-1}	6.6563E − 3	3.2670E − 3	1.6896E − 3	8.4847E − 4
2^{-2}	1.8844E − 2	1.0269E − 2	5.4071E − 3	2.7673E − 3
2^{-3}	4.4488E − 2	2.4705E − 2	1.3442E − 2	7.0005E − 3
2^{-4}	9.0864E − 2	4.4888E − 2	2.2601E − 2	1.2381E − 2
2^{-5}	1.1643E − 1	6.4920E − 2	3.3428E − 2	1.6773E − 2
2^{-6}	1.2614E − 1	7.3339E − 2	3.9266E − 2	2.0446E − 2
2^{-7}	1.3146E − 1	7.9200E − 2	4.3956E − 2	2.2509E − 2
2^{-8}	1.3425E − 1	8.2509E − 2	4.5454E − 2	2.3662E − 2
2^{-9}	1.3566E − 1	8.4256E − 2	4.6360E − 2	2.4324E − 2
2^{-10}	1.3638E − 1	8.5151E − 2	4.6846E − 2	2.4706E − 2
2^{-11}	1.3673E − 1	8.5600E − 2	4.7095E − 2	2.4907E − 2
2^{-12}	1.3690E − 1	8.5822E − 2	4.7217E − 2	2.5007E − 2
2^{-13}	1.3699E − 1	8.5930E − 2	4.7276E − 2	2.5055E − 2
2^{-14}	1.3703E − 1	8.5982E − 2	4.7304E − 2	2.5077E − 2
2^{-15}	1.3705E − 1	8.6008E − 2	4.7317E − 2	2.5088E − 2
2^{-16}	1.3706E − 1	8.6020E − 2	4.7323E − 2	2.5093E − 2
2^{-17}	1.3706E − 1	8.6026E − 2	4.7326E − 2	2.5096E − 2
2^{-18}	1.3706E − 1	8.6029E − 2	4.7328E − 2	2.5097E − 2
2^{-19}	1.3707E − 1	8.6031E − 2	4.7328E − 2	2.5097E − 2

ε	Number of Intervals N			
	128	256	512	1024
1	1.1368E − 4	5.5073E − 5	2.5717E − 5	1.1025E − 5
2^{-1}	4.2062E − 4	2.0419E − 4	9.5446E − 5	4.0939E − 5
2^{-2}	1.3807E − 3	6.7310E − 4	3.1532E − 4	1.3539E − 4
2^{-3}	3.5356E − 3	1.7335E − 3	8.1452E − 4	3.5028E − 4
2^{-4}	6.9735E − 3	3.4659E − 3	1.6398E − 3	7.0767E − 4
2^{-5}	8.4353E − 3	4.1872E − 3	1.9965E − 3	9.0290E − 4
2^{-6}	1.0330E − 2	5.1919E − 3	2.5176E − 3	1.1176E − 3
2^{-7}	1.1399E − 2	5.7018E − 3	2.7529E − 3	1.2171E − 3
2^{-8}	1.2081E − 2	6.0461E − 3	2.9070E − 3	1.2804E − 3
2^{-9}	1.2564E − 2	6.2754E − 3	3.0189E − 3	1.3265E − 3
2^{-10}	1.2797E − 2	6.4256E − 3	3.0958E − 3	1.3623E − 3
2^{-11}	1.2899E − 2	6.4984E − 3	3.1456E − 3	1.3879E − 3
2^{-12}	1.2952E − 2	6.5381E − 3	3.1740E − 3	1.4044E − 3
2^{-13}	1.2976E − 2	6.5570E − 3	3.1840E − 3	1.4112E − 3
2^{-14}	1.2987E − 2	6.5654E − 3	3.1883E − 3	1.4142E − 3
2^{-15}	1.2992E − 2	6.5691E − 3	3.1901E − 3	1.4155E − 3
2^{-16}	1.2995E − 2	6.5709E − 3	3.1909E − 3	1.4161E − 3
2^{-17}	1.2996E − 2	6.5717E − 3	3.1912E − 3	1.4163E − 3
2^{-18}	1.2996E − 2	6.5721E − 3	3.1913E − 3	1.4164E − 3
2^{-19}	1.2997E − 2	6.5722E − 3	3.1914E − 3	1.4165E − 3

Table 2. Maximum global errors $E^N_{\varepsilon,\text{global}}$ for the fitted mesh method $(\mathrm{P}^N_\varepsilon)$ applied to problem (5.1).

ε	Number of Intervals N			
	8	16	32	64
1	3.2571E − 3	1.2069E − 3	5.3242E − 4	2.4720E − 4
2^{-1}	8.4268E − 3	3.7600E − 3	1.8106E − 3	8.7879E − 4
2^{-2}	2.2307E − 2	1.0993E − 2	5.6245E − 3	2.8177E − 3
2^{-3}	4.9157E − 2	2.5897E − 2	1.3871E − 2	7.1129E − 3
2^{-4}	9.6434E − 2	4.5796E − 2	2.3243E − 2	1.2713E − 2
2^{-5}	1.2788E − 1	6.7233E − 2	3.3905E − 2	1.7014E − 2
2^{-6}	1.4223E − 1	7.8174E − 2	3.9632E − 2	2.0653E − 2
2^{-7}	1.5065E − 1	8.6360E − 2	4.5356E − 2	2.2721E − 2
2^{-8}	1.5534E − 1	9.1431E − 2	4.8127E − 2	2.3867E − 2
2^{-9}	1.5786E − 1	9.4357E − 2	4.9993E − 2	2.4516E − 2
2^{-10}	1.5921E − 1	9.5983E − 2	5.1134E − 2	2.5206E − 2
2^{-11}	1.5991E − 1	9.6867E − 2	5.1793E − 2	2.5739E − 2
2^{-12}	1.6027E − 1	9.7340E − 2	5.2161E − 2	2.6047E − 2
2^{-13}	1.6045E − 1	9.7582E − 2	5.2357E − 2	2.6214E − 2
2^{-14}	1.6055E − 1	9.7701E − 2	5.2454E − 2	2.6296E − 2
2^{-15}	1.6060E − 1	9.7759E − 2	5.2502E − 2	2.6336E − 2
2^{-16}	1.6063E − 1	9.7789E − 2	5.2525E − 2	2.6357E − 2
2^{-17}	1.6064E − 1	9.7803E − 2	5.2537E − 2	2.6367E − 2
2^{-18}	1.6065E − 1	9.7810E − 2	5.2543E − 2	2.6371E − 2
2^{-19}	1.6065E − 1	9.7814E − 2	5.2546E − 2	2.6374E − 2

ε	Number of Intervals N			
	128	256	512	1024
1	1.1784E − 4	5.6104E − 5	2.5974E − 5	1.1089E − 5
2^{-1}	4.2819E − 4	2.0608E − 4	9.5919E − 5	4.1057E − 5
2^{-2}	1.3942E − 3	6.7656E − 4	3.1618E − 4	1.3561E − 4
2^{-3}	3.5652E − 3	1.7414E − 3	8.1649E − 4	3.5077E − 4
2^{-4}	7.1137E − 3	3.5022E − 3	1.6491E − 3	7.1004E − 4
2^{-5}	8.5349E − 3	4.2235E − 3	2.0087E − 3	9.0698E − 4
2^{-6}	1.0428E − 2	5.2275E − 3	2.5301E − 3	1.1219E − 3
2^{-7}	1.1486E − 2	5.7369E − 3	2.7651E − 3	1.2210E − 3
2^{-8}	1.2172E − 2	6.0800E − 3	2.9192E − 3	1.2846E − 3
2^{-9}	1.2650E − 2	6.3089E − 3	3.0306E − 3	1.3303E − 3
2^{-10}	1.2880E − 2	6.4578E − 3	3.1074E − 3	1.3661E − 3
2^{-11}	1.2981E − 2	6.5300E − 3	3.1569E − 3	1.3919E − 3
2^{-12}	1.3032E − 2	6.5699E − 3	3.1852E − 3	1.4084E − 3
2^{-13}	1.3056E − 2	6.5890E − 3	1.1954E − 3	1.4151E − 3
2^{-14}	1.3067E − 2	6.5975E − 3	3.1997E − 3	1.4181E − 3
2^{-15}	1.3072E − 2	6.6014E − 3	3.2015E − 3	1.4194E − 3
2^{-16}	1.3074E − 2	6.6031E − 3	3.2022E − 3	1.4199E − 3
2^{-17}	1.3075E − 2	6.6039E − 3	3.2026E − 3	1.4201E − 3
2^{-18}	1.3076E − 2	6.6043E − 3	3.2027E − 3	1.4202E − 3
2^{-19}	1.3076E − 2	6.6045E − 3	3.2028E − 3	1.4203E − 3

Table 3. Estimated rates of convergence $p_{N,\varepsilon}$ and uniform rates p_N for the fitted mesh method $(\mathrm{P}_\varepsilon^N)$ applied to problem (5.1).

ε	Number of Intervals N						
	8	16	32	64	128	256	512
1	1.4380E + 0	9.5859E − 1	9.8879E − 1	9.9336E − 1	9.9753E − 1	9.9857E − 1	9.9936E − 1
2^{-1}	1.1158E + 0	9.1638E − 1	9.7415E − 1	9.8420E − 1	9.9303E − 1	9.9639E − 1	9.9822E − 1
2^{-2}	8.8184E − 1	8.7523E − 1	9.3777E − 1	9.6732E − 1	9.8386E − 1	9.9174E − 1	9.9589E − 1
2^{-3}	8.0470E − 1	8.0139E − 1	8.9924E − 1	9.4309E − 1	9.7142E − 1	9.8530E − 1	9.9261E − 4
2^{-4}	1.0073E + 0	1.0999E + 0	9.5546E − 1	6.4678E − 1	9.4415E − 1	9.7067E − 1	9.8493E − 1
2^{-5}	7.0615E − 1	9.0546E − 1	1.0150E + 0	9.8768E − 1	9.5767E − 1	9.9654E − 1	9.1094E − 1
2^{-6}	6.5627E − 1	8.3667E − 1	9.1406E − 1	9.7763E − 1	9.4660E − 1	9.3585E − 1	9.3153E − 1
2^{-7}	6.1219E − 1	6.8873E − 1	9.6181E − 1	9.6881E − 1	9.5512E − 1	9.4255E − 1	9.4355E − 1
2^{-8}	5.3404E − 1	7.3523E − 1	9.2699E − 1	9.4397E − 1	9.4950E − 1	9.4948E − 1	9.4926E − 1
2^{-9}	4.9653E − 1	7.5232E − 1	9.1958E − 1	9.0917E − 1	9.5462E − 1	9.4459E − 1	9.5198E − 1
2^{-10}	4.7817E − 1	7.6158E − 1	9.0748E − 1	9.0955E − 1	9.3975E − 1	9.4167E − 1	9.4829E − 1
2^{-11}	4.6909E − 1	7.6643E − 1	8.9819E − 1	9.1538E − 1	9.3555E − 1	9.3172E − 1	9.4272E − 1
2^{-12}	4.6457E − 1	7.6892E − 1	8.9369E − 1	9.1855E − 1	9.3314E − 1	9.2673E − 1	9.3798E − 1
2^{-13}	4.6232E − 1	7.7018E − 1	8.9148E − 1	9.2022E − 1	9.3037E − 1	9.2784E − 1	9.3558E − 1
2^{-14}	4.6120E − 1	7.7082E − 1	8.9039E − 1	9.2108E − 1	9.2907E − 1	9.2859E − 1	9.3484E − 1
2^{-15}	4.6064E − 1	7.7114E − 1	8.8985E − 1	9.2152E − 1	9.2844E − 1	9.2902E − 1	9.3402E − 1
2^{-16}	4.6035E − 1	7.7130E − 1	8.8958E − 1	9.2174E − 1	9.2813E − 1	9.2926E − 1	9.3365E − 1
2^{-17}	4.6021E − 1	7.7138E − 1	8.8944E − 1	9.2185E − 1	9.2798E − 1	9.2938E − 1	9.3349E − 1
2^{-18}	4.6014E − 1	7.7142E − 1	8.8937E − 1	9.2190E − 1	9.2790E − 1	9.2945E − 1	9.3341E − 1
2^{-19}	4.6011E − 1	7.7144E − 1	8.8934E − 1	9.2193E − 1	9.2787E − 1	9.2948E − 1	9.3337E − 1
p_N	4.6011E − 1	7.7144E − 1	8.8934E − 1	9.2193E − 1	9.2787E − 1	9.2948E − 1	9.3337E − 1

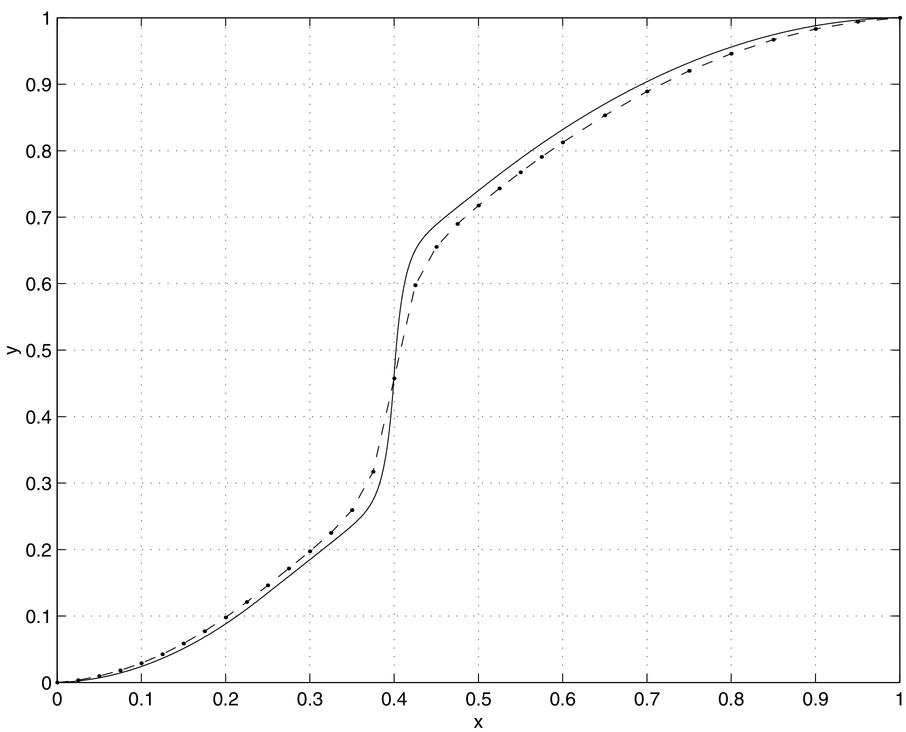

(a). $\tilde{U}_{0.01}^{32}$ (- -), $\tilde{U}_{0.01}^{4096}$ (—).

Figure 4. Plots of the numerical solution $\tilde{U}_\varepsilon^N$, computed on a uniform mesh, and the continuous solution u_ε, for $\varepsilon = 0.01$ and $\varepsilon = 0.0001$, respectively, with $N = 32$.

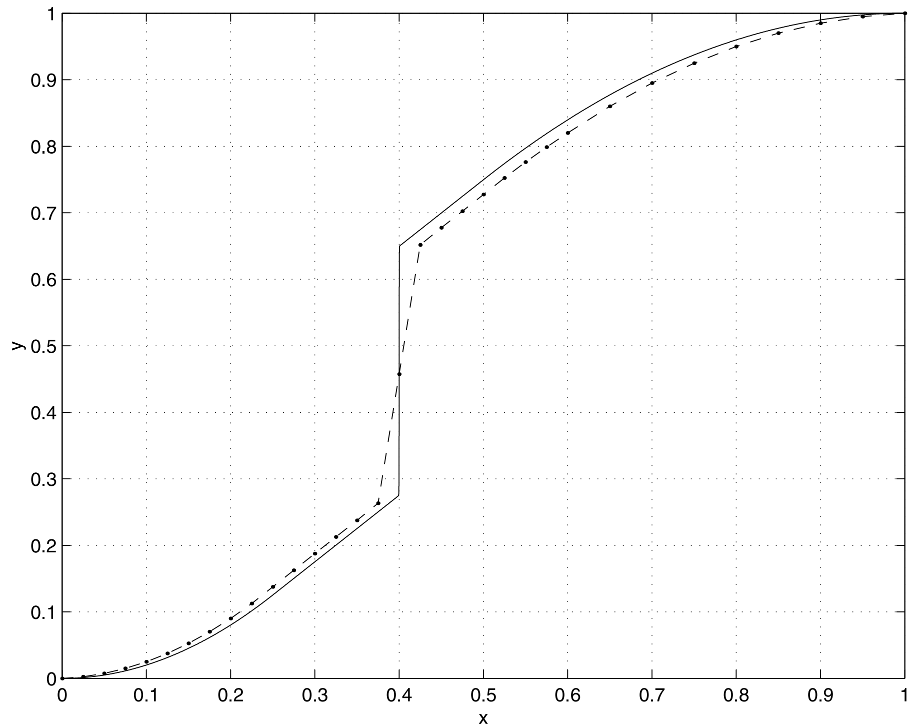

(b). $\tilde{U}^{32}_{0.0001}$ (- -), $\tilde{U}^{4096}_{0.0001}$ (—).

Figure 4. (cont.)

The evident waves in these plots depict the increase in the error between mesh points of the mesh $\Omega^{32}_{\varepsilon}$.

The differences between the numerical solutions for various values of N and the numerical solution for $N = 4096$, which are indicative of the nodal errors, are presented in Table 1.

Orders of convergence of the numerical solutions, estimated from the ratios of the two mesh differences, as in [3] are presented in Table 3. They bear out the theoretical results given above in Theorem 7.

Figure 4 shows the numerical solutions $\tilde{U}^N_{\varepsilon}$ obtained using standard upwinding L^N_{ε} on a uniform mesh

$$\Omega^N_{\text{unif}} = \left\{ x_i : x_i = \frac{i}{N},\ 1 \le i \le N-1 \right\}, \tag{5.2}$$

with $N + 32$, for $\varepsilon = 0.01$ and $\varepsilon = 0.0001$.

The differences between the numerical solutions obtained using standard upwinding on uniform meshes Ω^N_{unif}, for various values of N, and the numerical solution on the piecewise uniform mesh $\Omega^{4096}_{\varepsilon}$, which are again indicative of the nodal errors for these meshes, are presented in Table 4.

Observe in Table 4 that in the region where $\varepsilon N \le 0.25$, the maximum pointwise errors actually increase as the mesh is refined. This indicates that the method is not ε-uniform. This undesirable behaviour should be contrasted with the corresponding entries in Table 1. In Table 1, the maximum pointwise errors decrease as the mesh is refined irrespective of size of ε. Note also that the maximum pointwise errors are being measured at different mesh points in Tables 1 and 4. In Table 1, half of the mesh points in the fitted mesh method are always located within the layer region. In Table 4, for $\varepsilon N \le 0.25$, the mesh points on the uniform mesh are located only in the smooth regions outside the interior layers.

Table 4. Maximum pointwise errors $E^N_{\varepsilon,\mathrm{nodal}}$ for standard upwinding on uniform meshes applied to problem (5.1).

ε	Number of Intervals N			
	8	16	32	64
1	4.3407E − 3	1.5301E − 3	6.5766E − 4	3.0250E − 4
2^{-1}	1.0721E − 2	4.5160E − 3	2.1639E − 3	1.0490E − 3
2^{-2}	2.5803E − 2	1.2606E − 2	6.4248E − 3	3.2271E − 3
2^{-3}	5.2045E − 2	2.7637E − 2	1.4466E − 2	7.3961E − 3
2^{-4}	7.7957E − 2	4.2938E − 2	2.2837E − 2	1.1742E − 2
2^{-5}	9.8480E − 2	5.7780E − 2	3.2267E − 2	1.7115E − 2
2^{-6}	9.9740E − 2	6.8632E − 2	4.6194E − 2	2.6167E − 2
2^{-7}	9.5653E − 2	6.2928E − 2	5.3016E − 2	4.0122E − 2
2^{-8}	9.2892E − 2	5.4902E − 2	4.4089E − 2	4.4923E − 2
2^{-9}	9.1354E − 2	5.0066E − 2	3.4245E − 2	3.4470E − 2
2^{-10}	9.0544E − 2	4.7456E − 2	2.8489E − 2	2.3805E − 2
2^{-11}	9.0129E − 2	4.6099E − 2	2.5417E − 2	1.7642E − 2
2^{-12}	8.9919E − 2	4.5408E − 2	2.3830E − 2	1.4368E − 2
2^{-13}	8.9813E − 2	4.5059E − 2	2.3023E − 2	1.2680E − 2
2^{-14}	8.9760E − 2	4.4883E − 2	2.2616E − 2	1.1823E − 2
2^{-15}	8.9734E − 2	4.4795E − 2	2.2412E − 2	1.1391E − 2
2^{-16}	8.9720E − 2	4.4751E − 2	2.2310E − 2	1.1174E − 2
2^{-17}	8.9714E − 2	4.4729E − 2	2.2258E − 2	1.1066E − 2
2^{-18}	8.9710E − 2	4.4718E − 2	2.2233E − 2	1.1012E − 2
2^{-19}	8.9709E − 2	4.4713E − 2	2.2220E − 2	1.0984E − 2

ε	Number of Intervals N			
	128	256	512	1024
1	1.4348E − 4	6.8456E − 5	3.2035E − 5	1.4099E − 5
2^{-1}	5.1088E − 4	2.4699E − 4	1.1629E − 4	5.1274E − 5
2^{-2}	1.6020E − 3	7.8165E − 4	3.6933E − 4	1.6267E − 4
2^{-3}	3.7052E − 3	1.8139E − 3	8.5614E − 4	3.7453E − 4
2^{-4}	5.8812E − 3	2.8633E − 3	1.3300E − 3	5.5965E − 4
2^{-5}	8.8194E − 3	4.3420E − 3	2.0142E − 3	8.2851E − 4
2^{-6}	1.4354E − 2	7.3913E − 3	3.6086E − 3	1.6318E − 3
2^{-7}	2.2925E − 2	1.2889E − 2	6.6230E − 3	3.2170E − 3
2^{-8}	3.6981E − 2	2.1245E − 2	1.2133E − 2	6.2558E − 3
2^{-9}	4.0794E − 2	3.5382E − 2	2.0387E − 2	1.1747E − 2
2^{-10}	2.9607E − 2	3.8705E − 2	3.4572E − 2	1.9951E − 2
2^{-11}	1.8556E − 2	2.7158E − 2	3.7651E − 2	3.4162E − 2
2^{-12}	1.2204E − 2	1.5921E − 2	2.5926E − 2	3.7119E − 2
2^{-13}	8.8360E − 3	9.4809E − 3	1.4594E − 2	2.5306E − 2
2^{-14}	7.1016E − 3	6.0681E − 3	8.1165E − 3	1.3903E − 2
2^{-15}	6.2213E − 3	4.3113E − 3	4.6836E − 3	7.4245E − 3
2^{-16}	5.7778E − 3	3.4199E − 3	2.9160E − 3	3.9894E − 3
2^{-17}	5.5553E − 3	2.9709E − 3	2.0191E − 3	2.2173E − 3
2^{-18}	5.4438E − 3	2.7455E − 3	1.5673E − 3	1.3182E − 3
2^{-19}	5.3879E − 3	2.6326E − 3	1.3406E − 3	8.6534E − 4

6. CONCLUSION

A singularly perturbed convection-diffusion problem, with a discontinuous convection coefficient and a singular perturbation parameter ε, was examined. Due to the discontinuity an interior layer appears in the solution. A finite difference method was constructed for solving this problem, which generates ε-uniformly convergent numerical approximations to the solution. The method uses a piecewise uniform mesh, which is fitted to the interior layers, and the standard upwind finite difference operator on this mesh. The main theoretical result is the ε-uniform convergence in the global maximum norm of the approximations generated by this finite difference method. Numerical results were presented, which are in agreement with the theoretical results.

REFERENCES

1. K.W. Morton, *Numerical Solution of Convection Diffusion Problems*, Chapman and Hall, London, (1995).
2. E.P. Doolan, J.J.H. Miller and W.H.A. Schilders, *Uniform Numerical Methods for Problems with Initial and Boundary Layers*, Boole Press, Dublin, (1980).
3. P.A. Farrell, A.F. Hegarty, J.J.H. Miller, E. O'Riordan and G.I. Shishkin, *Robust Computational Techniques for Boundary Layers*, Chapman and Hall/CRC, Boca Raton, FL, (2000).
4. H.-G. Roos, M. Stynes and L. Tobiska, *Numerical Methods for Singularly Perturbed Differential Equations. Convection-Diffusion and Flow Problems*, Springer-Verlag, New York, (1996).
5. G.I. Shishkin, Discrete approximation of singularly perturbed elliptic and parabolic equations, Russian Academy of Sciences, Ural Section, Ekaterinburg (in Russian), (1992).
6. P.A. Farrell, A.F. Hegarty, J.J.H. Miller, E. O'Riordan and G.I. Shishkin, Singularly perturbed differential equations with discontinuous source terms, In *Analytical and Numerical Methods for Convection-Dominated and Singularly Perturbed Problems*, (Edited by J.J.H. Miller, G.I. Shishkin and L. Vulkov), pp. 23–32, Nova Science, New York, (2000).
7. P.A. Farrell, A.F. Hegarty, J.J.H. Miller, E. O'Riordan and G.I. Shishkin, Singularly perturbed convection diffusion problems with boundary and weak interior layers, DCU School of Mathematics Preprint, Ms-01-07, (2001).